Preprints of the 21st IFAC World Congress (Virtual)
Berlin, Germany, July 12-17, 2020

A Minimal Set of Sensors in a Smart-Shirt to Obtain Respiratory Parameters

B. Laufer*, R. Murray, P. D. Docherty**, S. Krueger-Ziolek*, F. Hoeflinger***, L. Reindl*** and K. Moeller***

** Institute of Technical Medicine (ITeM), Furtwangen University, Villingen-Schwenningen, Germany (Tel: +49 7720 3074621; e-mail: b.laufer@hs-furtwangen.de)*
*** University of Canterbury, Christchurch, New Zealand*
**** Department of Microsystems Engineering, University of Freiburg, Freiburg, Germany*

Abstract: Smart-Shirts (and other wearable technologies) that provide vital medical data are becoming increasingly prevalent. However, obtaining accurate measurement of respiratory parameters via a Smart-Shirt requires ongoing research. In this study, various respiratory parameters have been captured via an optoelectronic plethysmograph and a body plethysmograph using an optimal set of spatial sensors. Sixty-four reflective markers were fixed on a compression shirt and different respiratory manoeuvres were performed by the subjects. In this analysis, Singular Value Decomposition was used to determine the minimum marker set required to yield accurate predictions of respiratory mechanics. Sufficient accuracy and precision for most clinical applications was able to be determined using positional data from nine markers. Using motions of nine sensors, the tidal volume can be predicted with a mean error of less than 139 ml and an adjusted R^2 higher than 0.96. A subsequent linear regression analysis provides the location of the nine markers. These outcomes reduce the computational complexity of analysing optical based wearable technology, reducing barriers to further uptake.

Keywords: Position Sensors, Tidal volume, Respiratory Parameters, Sensor Location, Wearables

1. INTRODUCTION

The increase in air pollution and life expectancy of the human population correlates with increased pulmonary disease (Barnes et al. 2014, Ferkol and Schraufnagel 2014). Therefore, low-cost monitoring of respiratory parameters that reflect the health of lungs will become more significant.

In spontaneous breathing, these parameters are typically determined via gold-standard pulmonary function tests: spirometry or body plethysmography (C.-P. Criée 2015, Coates et al. 1997, Criée et al. 2011, Hayes and Kraman 2009, Miller et al. 2005). Unfortunately, both systems have the disadvantage that the subject must breathe through a facemask or a mouthpiece, while the nasal passage is blocked by a clip. These measurements can be uncomfortable for the subject, especially during longer measurements or during exercise.

Therefore, the aim of this study is to obtain tidal volume via the surface motion of the upper body. This idea was initially proposed by Konno and Mead (Konno and Mead 1967). Subsequently, multiple studies have been carried out analysing surface motions of the upper body as a surrogate for spirometry or body plethysmography in the determination of respiratory parameters (Cala et al. 1996, De Groote et al. 1985, Ferrigno et al. 1985). However, an accurate wearable system is still not available on the market.

Optoelectronic plethysmography (OEP) showed the potential to meet the objective (Massaroni et al. 2017, Parreira et al. 2012, Romagnoli et al. 2008, Vogiatzis et al. 2005). OEP uses cameras to measure the spatial positions of reflective markers to determine surface motion of the upper body. The method can provide sophisticated measurements in clinical settings and research. However, OEP is very expensive to operate and measurement is restricted to movements within the area between the cameras.

Currently, due to the development of improved, novel and miniaturized sensors, wearable technologies are on the rise (Chu et al. 2019, Ciocchetti et al. 2015, Gaidhani et al. 2017, Hering and Schönfelder 2012, Karacocuk et al. 2019, Yang 2014). Smart-Shirts are getting increased attention in research and development (Aliverti 2017, Heyde et al. 2015). Smart-Shirts that can measure vital parameters, such as heart or respiratory rate, are currently available on the market, but a Smart-Shirt that provides other respiratory parameters such as accurate tidal volume, cannot be found. Such a Smart-Shirt would be beneficial for various clinical tasks and in high level sports.

The number of sensors is a decisive factor in the development of Smart-Shirts. A high number of sensors might improve the accuracy of the measurement, but will also increase cost, size and complexity of the Smart-Shirt. Therefore, a fundamental objective of Smart-Shirt development is to optimise the number of sensors to provide the lowest level of discomfort, complexity and cost while ensuring the desired system accuracy.

Previous approaches have attempted to determine the minimal number of position sensors in various ways (Laufer et al. 2017, Laufer et al. 2018). However, this study analyses

the optimal number and location of spatial sensors, using the information content of each sensor signal to find optimal sensor placement for tidal volume measurement.

2. METHODS

2.1 Data

This study uses data from Laufer et al. (Laufer, et al. 2018), where breaths of varying tidal volumes were performed by three volunteers.

The measurement was done with a constant-volume body plethysmograph (PowerCube® Body+, Ganshorn Medizin Electronic, Germany) which was surrounded by 9 infrared motion tracking cameras (VICON Bonita B10, Firmware Version 404) of an OEP system. The OEP was a camera-based motion tracking-system (Bonita, VICON, Denver, CO) with a sampling frequency of 100 Hz. The measurement setup can be seen schematically in Fig. 1.

Sixty-four motion tracking markers were fixed to a compression shirt at different heights (Fig. 2). Thirty-two markers were fixed ventral to the shirt, 26 dorsal and 6 markers were fixed lateral (3 markers at each side of the shirt).

The data transfer from the VICON system to MATLAB (R2019a, The MathWorks, Natick, USA) was done with the VICON Nexus Software (Version 1.8.5.6 1009h, Vicon Motion Systems Ltd.). All further data processing was done with MATLAB.

The body plethysmograph gave access to flow, mouth pressure and the cabin pressure data with a sampling frequency of 200 Hz. LF8 software (Version 8.5M RC25r7071, Ganshorn Medizin Electronic GmbH) was used for data recording. The raw data of the body plethysmograph was obtained via the serial port.

Details to the subjects can be found in Table 1 and respiratory manoeuvres are listed in Table 2.

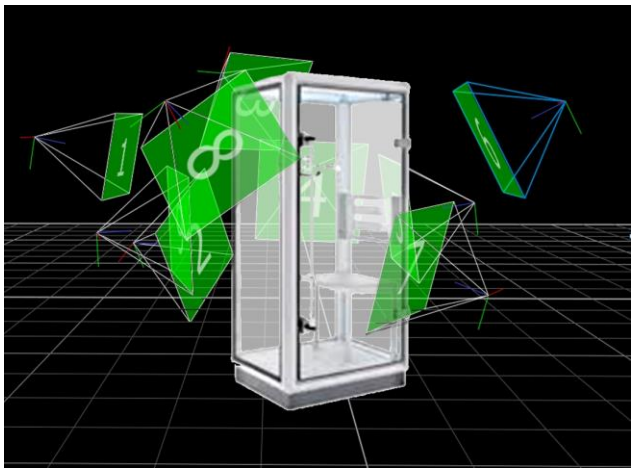

Fig. 1. Measurement setup: body plethysmograph surrounded by the cameras of the motion tracking system. (figure published 2018 in *Laufer et al.)*

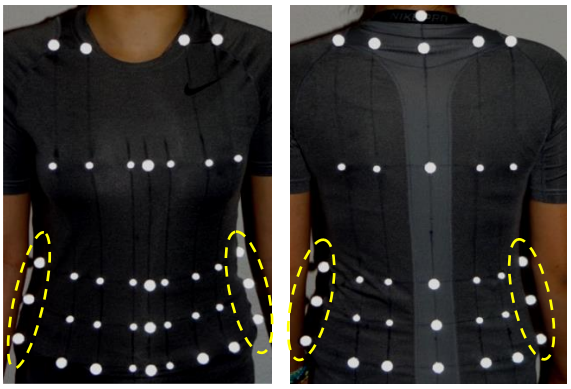

Fig. 2: Motion tracking markers, fixed on a compression shirt (front / ventral view (left) and back / dorsal view (right)). Here, the lateral markers are marked by thin dashed yellow ellipses. (figure published 2018 in *Laufer et al.)*

The number n of measurement points in time was about 21.000 but n was dependent on the breathing rhythm and varied from subject to subject. For exhaustive details on the experimental procedure please refer to Laufer et al. (2018).

Table 1. Participants

Subject	Height (m)	Weight (kg)	Gender	BMI (kg/m^2)	Age (years)
1	1.82	66	male	19.9	25
2	1.84	76	male	22.4	27
3	1.60	48	female	18.8	32

Table 2. Respiratory manoeuvres

Approximate duration	Respiration manoeuvre
30 seconds	normal spontaneous breathing
30 seconds	3 deeper breaths
30 seconds	normal spontaneous breathing
30 seconds	3 maximal breaths
30 seconds	normal spontaneous breathing
30 seconds	shallow breathing
30 seconds	normal spontaneous breathing

2.2 Data processing

Fig. 3 illustrates the processing-workflow of the spatial position data, provided by reflective marker movement of an OEP with the aim to get optimal location and number of markers/sensors for the Smart-Shirt.

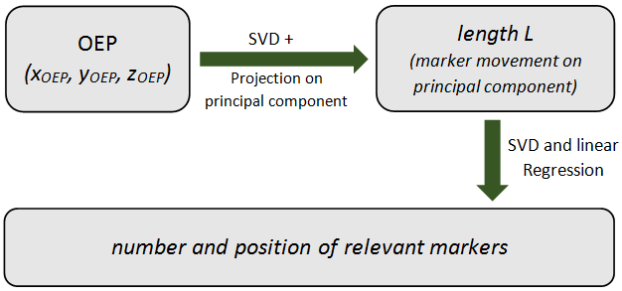

Fig. 3. Data processing via Singular Value Decomposition SVD and linear regression.

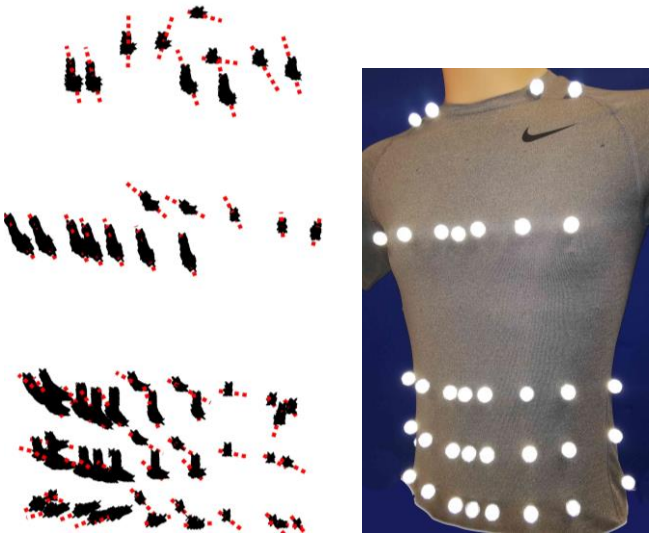

Fig. 4. Position data (black) over time during various respiratory manoeuvres are illustrated based on the data of subject 1 (left), where the position data are nearly in line (red dotted lines). The corresponding compression shirt with reflective markers is shown (right).

Initial exploration of the data showed that the movement of individual markers was not particularly distinctive, and that each marker was moving predominantly on a particular line (see Fig. 4). Hence, a dimension reduction could be undertaken. Separately for each of the j markers (with $1 \leq j \leq 64$), the mean position value $(\overline{x_{OEP}}, \overline{y_{OEP}}, \overline{z_{OEP}})_j$ of the movement of marker j was calculated and the movement was referenced from the obtained mean value.

$$(x, y, z)_{t_i,j} = (x_{OEP}, y_{OEP}, z_{OEP})_{t_i,j} - (\overline{x_{OEP}}, \overline{y_{OEP}}, \overline{z_{OEP}})_j \quad (1)$$

Afterwards, the position data during the measurement $(x,y,z)_j$ were projected on the direction of their main principal component vector (see Fig. 5). This principal component was obtained by using a Singular Value Decomposition (SVD).

$$U\Sigma V^* = svd\begin{bmatrix} x_{t_1} & y_{t_1} & z_{t_1} \\ \vdots & \vdots & \vdots \\ x_{t_n} & y_{t_n} & z_{t_n} \end{bmatrix} \quad (2)$$

where: t_1 to t_n are all time-points of the measurement. Then let L_j be the projection of $(x,y,z)_j$ onto the first column of V^*_j. The measured spatial positions (x_{OEP}, y_{OEP}, z_{OEP}) can be approximated by

$$(x_{OEP}, y_{OEP}, z_{OEP})_{t_i,j} \approx (\overline{x_{OEP}}, \overline{y_{OEP}}, \overline{z_{OEP}})_j + L_{t_i,j} V^*_{1,j} \quad (3)$$

(L_j is the length of the movement of marker j in direction of its principal component and $V^*_{1,j}$ is the unit vector of the main principal component of marker j).

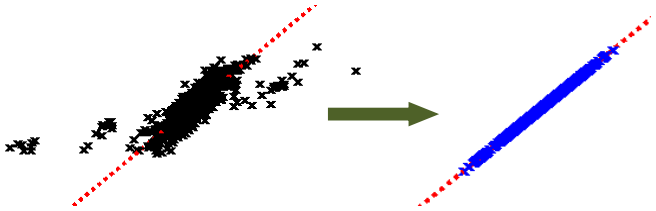

Fig. 5. Dimension reduction by the projection of the position data (black) on the principal component line (red) of one marker, while the projected positions are illustrated in blue.

After this dimension reducing, the information content of the system was analysed via a further SVD:

$$U\Sigma V^* = svd[M] \text{ where: } M = \begin{bmatrix} L_{1,t_1} & \cdots & L_{64,t_1} \\ \vdots & \ddots & \vdots \\ L_{1,t_n} & \cdots & L_{64,t_n} \end{bmatrix} \quad (4)$$

where: U is an orthogonal 64×64 rotation matrix, Σ a diagonal $64\times n$ stretching matrix and V^* an orthogonal $n\times n$ rotation matrix and n the number of time-points. M is the matrix of length vectors of all markers.

The column vectors of Σ are the singular vectors of M, sorted in information content, so that the vector carrying most information is the first column vector. Thus, by analysing these singular vectors the number of vectors k can be determined, in order to achieve the required accuracy of the system refer to the principal components (see Fig. 6). Thus, the number of principal components which carried more than 2% of the total system information was selected. This number can serve as a guide for the number of markers needed regarding the initial, non-rotated system. Furthermore, several markers are considered to be essential for correction of movements that are not respiration induced: the reference markers at the cervical, the middle and the lowest spine. Twists and bending of the upper body can captured by the movement of these 3 markers and thus, the 3 markers were fixed in the reduced marker set. At least k markers were necessary to get the desired system accuracy in the real-world system. Thus, k+3 markers were taken into consideration for the measurement system.

After the number of markers was specified, a linear regression analysis showed which of the reflective markers carried most of the information. The results were calculated using the *backslash* function of MATLAB.

$$\lambda = M \backslash V_{body} \text{ (equivalent to } \lambda = (M^T M)^{-1} M^T V_{body}) \quad (5)$$

Where: V_{body} was the volume, measured by the body plethysmograph.

After regression, λ was sorted. The higher the corresponding λ-value of a marker, the higher the sensitivity of the system refer to this marker. Thus, additional to the three essential markers, k markers with the highest λ–values were used for further calculation.

Via a bootstrapping algorithm on each measurement, the best sensor locations were analysed. For each subject, the data of 500 randomly chosen sections of the experimental data were analysed. The number of times each marker represented more

than 2% of the system information was counted. A threshold of 2% was arbitrarily chosen as it was estimated that this value would yield good agreement between the predictions of the approach and the measured data. Then each marker that contributed less than 50 times (10% of the 500 analysis) amongst all subjects to the system information, were neglected.

Subsequently, the bootstrapping was repeated on the reduced marker set with 1000 repetitions. Based on the bootstrapping data, the optimal markers were chosen from the marker set. These markers contributed the most to the system information and were necessary for the model. Finally, the marker set was reduced further to k+3 markers while minimising the disagreement between the respiratory parameters predicted by the markers and the volume data from the body plethysmograph.

3. RESULTS

The number of principal components and their corresponding information content of the system can be seen in Fig. 6. All principal components that contained more than 2% of the system information were selected for further calculation. Amongst all three subjects, k = 6 principle components had more than 2% of system information and therefore, the corresponding number of markers / sensors, which was used for further calculation was set to 9 (k + 3 = 9).

Linear regression combined with a bootstrapping algorithm allowed identification of the optimal markers from the marker set shown in figure 7. The information of the marker set of the optimal markers compared to the volume data of the body plethysmograph (mean squared error and the adjusted R^2) is shown in Table 3. Figure 8 shows the result of the marker set based on the data of subject 1, after the determination of the λ-values by linear regression (according to equation 5 but based on the optimal 9 markers).

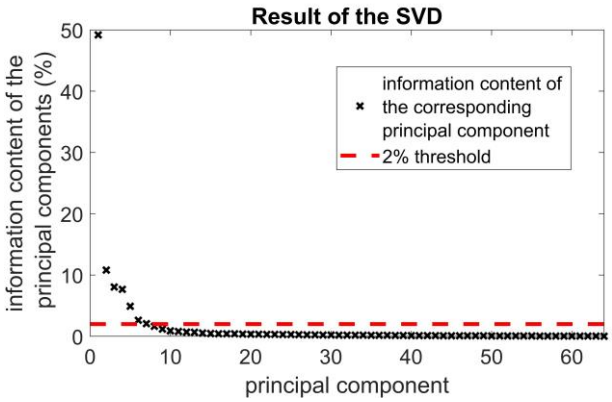

Fig. 6. A result of the SVD – the number of principal components and the corresponding information content of the system, illustrated based on the data of subject 2.

Table 3. Measurement results

Subject	$error_{mean}$ (ml)	adjusted R^2
1	82.5	0.984
2	138.6	0.965
3	71.4	0.982

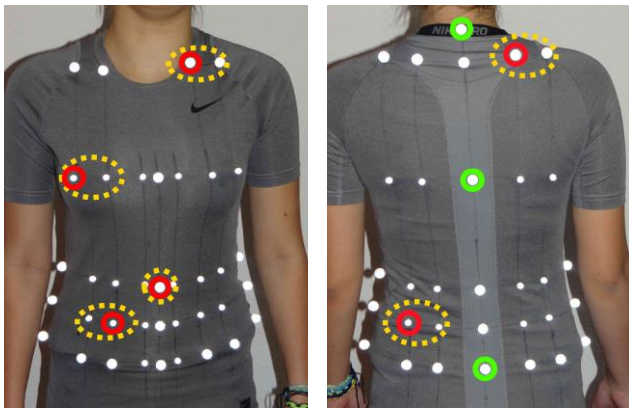

Fig. 7. Nine markers used for this calculation. The 3 fixed markers (green) and the 6 selected markers (red). The yellow ellipses show areas, where either marker could be selected.

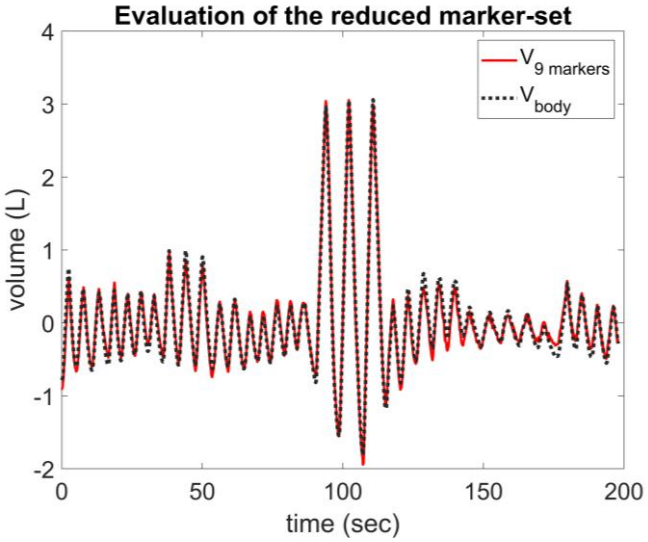

Fig. 8. Volumes, given by the body plethysmograph and the volume calculated with 9 sensors, illustrated based on the data of subject 1.

4. DISCUSSION

The OEP delivers accurate position information of the reflective markers. However, initial investigation of the motion of the markers showed that the information from most markers was redundant. In particular, the markers generally moved in unison and the individual markers generally moved on a particular line. Hence, this study aimed to reduce the cost and analysis complexity for estimating respiratory parameters from optical measurements by reducing the size of the data set required.

The resulting marker set is shown in Fig. 7. Due to symmetry and similarity of adjacent markers most markers in the optimal set could be replaced with proximal markers (yellow ellipses in Fig. 7). However, the low precision needed for the marker placement does not imply that an entirely arbitrary set of nine marker placements would yield accurate respiratory mechanics. In contrast, this analysis showed that the general placement across the thorax required to capture accurate and precise respiratory mechanics. The non-uniqueness of markers in each of the regions shown in figure 7 allowed the SVD analyses to obtain the reduced marker distribution that

contained the most unique information. In particular, the SVD analysis enabled the generation of a grey-box model that captured global motions of the chest via a limited set of local measurements.

The SVD methodology used enabled very good correlation between the measured volume data and a heavily reduced marker set. In particular, reducing from 64 markers to nine allowed $R^2 > 0.96$ for the three participants tested (Table 3). Furthermore, there were no noticeable aberrations from the measured data (Figure 8). This indicates that the methodology did not include systemic bias that may reduce the clinical value of the overall approach. This is an important factor for use in practice as it may be expected that changes in breathing patterns would be of primary interest to inform decision-support in critical care or high-performance sports training.

SVD is a well-known method for determining the key contributors to a particular behaviour. However, it can also be used to determine how to use a reduced data set to predict the behaviour. This research yielded parameter coefficients that can be used to predict respiratory mechanics from the motion of a few motion sensors on the chest. Further research is required to determine how applicable these coefficient values are across individuals and if calibration is required when the system is used for the first time or when patient condition changes.

This study exploited this benefit by determining the markers that contained more than 2% unique information about the system behaviour. While this was an arbitrary choice, it yielded a level of agreement that was sufficiently high to be of use in a clinical setting. Figure 6 shows how alterations to the 2% threshold would affect the number of parameters in the analysis. Shifting to 10% information content would lead to only two markers (in addition to the three datum markers). These markers would capture broad trends in the chest and stomach breathing, respectively. In contrast lowering the threshold to 1% would increase the number of markers to 16 but would also potentially increase the level of agreement between the predictions of the approach and the measured data. Further consideration is required to determine the optimal number of parameters for any given scenario.

For clinical applications, the patient is generally supine, and there are only minimal lateral or torsional movements of the spine. Hence, there would not be movements in the lung that confound the approach shown in this analysis. However, most sporting applications require a significant range of motion in the thorax, potentially confounding this approach. The addition of further markers that can capture this motion would theoretically allow information that could be used to mitigate the effects of these motions. However, the lung has a complex geometry and it is unlikely that the linear assumptions of this SVD approach would be able to capture the expected non-linear effects of complex motions of the spine on respiratory mechanics. Further research is required to confirm the contribution of lateral and torsional motion of the lung.

Two bootstrapping algorithms were applied one after the other, to analyse the best sensor locations amongst all the three subjects. The first bootstrapping helped to reduce the marker set further. All markers, which contribute less than 10% of all analysis of the bootstrapping to the system information amongst all three subjects, were omitted from further analysis. Another more precise bootstrapping approach reduced the set of 40 candidate markers from the first bootstrap to an optimised set of the nine markers that consistently contribute the most to volume estimation correlation with the body plethysmograph. The 2-stage approach used in this analysis was required to quickly determine the optimal marker set. The second stage could potentially have been used in isolation. However, this stage was much slower to converge and converging from 64 markers to six in a single approach would have been computationally onerous. Previous work has shown the robustness of hierarchical identification (Schranz et al. 2011).

This analysis used only three data sets from three healthy young individuals. This study analysed the optimal location and number of sensors for different tidal volume manoeuvres. Future work should evaluate the results additionally in different breathing manoeuvres, such as chest and abdominal breathing and in different breathing speed (e.g. panting). It would seem most likely that the finding would not be applicable in chronic obstructive pulmonary disease or in cases wherein a general symmetry in lung behaviour should not be assumed. In such cases, the viscoelastic behaviour of the lung in non-linear and even calibration is unlikely to improve the outcomes. The use of surface motion of the thorax may still allow prediction of respiratory mechanics in these cases. However, it is most likely that nonlinear mechanics transforms will be required if a similar SVD approach is used.

Nonetheless, there remain very many cases wherein the proposed methodology shows considerable promise. In particular, the approach is imminently applicable to very accurate measurement of the respiratory behaviour of sedate, supine patients with very low levels of intrusion. Only visual analysis of the patient's thorax motion would be required. Further analysis and development are required before this can be used for analysis of respiratory patterns in sporting applications.

5. CONCLUSION

The optimal number and the location of markers / sensors to obtain tidal volume were identified using a SVD approach. This study showed that the main information of the measurement system can be captured with a set of nine markers with sufficient accuracy (adjusted R^2 higher than 0.96) to imply that it may enable future use in clinical applications.

ACKNOWLEDGEMENT

This work was partially supported by the German Federal Ministry of Education and Research (MOVE, Grant 13FH628IX6) and H2020 MCSA Rise (#872488 — DCPM).

AUTHOR'S STATEMENT

Research funding: As mentioned in the Acknowledgments public funded grants are involved. Conflict of interest:

Authors state no conflict of interest. Informed consent: Informed consent has been obtained from all individuals included in this study. Ethical approval: The research related to human use complies with all the relevant national regulations, institutional policies and was performed in accordance with the tenets of the Helsinki Declaration, and has been approved by the authors' institutional review board or equivalent committee.

REFERENCES

Aliverti, A. (2017). Wearable technology: role in respiratory health and disease. *Breathe (Sheff),* vol. 13 (2), pp. e27-e36.

Barnes, P. J., Blasi, F., Ward, B., Reeves, E., and Rabe, K. F. (2014). Respiratory diseases in the world: one voice "united for lung health". *European Respiratory Journal,* vol. 43 (1), pp. 3-5.

C.-P. Criée, X. B., D. Berdel et al. (2015). Leitlinie zur Spirometrie. *Pneumologie,* vol. 69(03), pp. 147-64.

Cala, S. J., Kenyon, C. M., Ferrigno, G., Carnevali, P., Aliverti, A., Pedotti, A., Macklem, P. T., and Rochester, D. F. (1996). Chest wall and lung volume estimation by optical reflectance motion analysis. *Journal of Applied Physiology,* vol. 81 (6), p. 2680.

Chu, M., Nguyen, T., Pandey, V., Zhou, Y., Pham, H. N., Bar-Yoseph, R., Radom-Aizik, S., Jain, R., Cooper, D. M.*, et al.* (2019). Respiration rate and volume measurements using wearable strain sensors. *npj Digital Medicine,* vol. 2 (1), p. 8.

Ciocchetti, M., Massaroni, C., Saccomandi, P., Caponero, M. A., Polimadei, A., Formica, D., and Schena, E. (2015). Smart Textile Based on Fiber Bragg Grating Sensors for Respiratory Monitoring: Design and Preliminary Trials. *Biosensors,* vol. 5 (3), pp. 602-15.

Coates, A. L., Peslin, R., Rodenstein, D., and Stocks, J. (1997). Measurement of lung volumes by plethysmography. *European Respiratory Journal,* vol. 10 (6), p. 1415.

Criée, C. P., Sorichter, S., Smith, H. J., Kardos, P., Merget, R., Heise, D., Berdel, D., Köhler, D., Magnussen, H.*, et al.* (2011). Body plethysmography – Its principles and clinical use. *Respiratory Medicine,* vol. 105 (7), pp. 959-71.

De Groote, A., Wantier, M., Cheron, G., Estenne, M., and Paiva, M. (1985). Chest wall motion during tidal breathing. *J Appl Physiol,* vol. 83 (5), pp. 1531-7.

Ferkol, T. and Schraufnagel, D. (2014). The global burden of respiratory disease. *Ann Am Thorac Soc,* vol. 11 (3), pp. 404-6.

Ferrigno, G., Carnevali, P., Aliverti, A., Molteni, F., Beulcke, G., and Pedotti, A. (1985). Three-dimensional optical analysis of chest wall motion. *J Appl Physiol,* vol. 77 (3), pp. 1224-31.

Gaidhani, A., Moon, K. S., Ozturk, Y., Lee, S. Q., and Youm, W. (2017). Extraction and Analysis of Respiratory Motion Using Wearable Inertial Sensor System during Trunk Motion. *Sensors (Basel),* vol. 17 (12).

Hayes, D. and Kraman, S. S. (2009). The physiologic basis of spirometry. *Respiratory Care,* vol. 54 (12), pp. 1717-26.

Hering, E. and Schönfelder, G. (2012). *Sensoren in Wissenschaft und Technik : Funktionsweise und Einsatzgebiete,* Available: http://dx.doi.org/10.1007/978-3-8348-8635-4

Heyde, C., Mahler, H., Roecker, K., and Gollhofer, A. (2015). A wearable respiratory monitoring device--the between-days variability of calibration. *Int J Sports Med,* vol. 36 (1), pp. 29-34.

Karacocuk, G., Höflinger, F., Zhang, R., Reindl, L. M., Laufer, B., Möller, K., Röell, M., and Zdzieblik, D. (2019). Inertial Sensor-Based Respiration Analysis. *IEEE Transactions on Instrumentation and Measurement*, pp. 1-8.

Konno, K. and Mead, J. (1967). Measurement of the separate volume changes of rib cage and abdomen during breathing. *J Appl Physiol,* vol. 22 (3), pp. 407-22.

Laufer, B., Kretschmer, J., Docherty, P. D., Möller, K., Höflinger, F., and Reindl, L. (2017). Sensor placement in a smart compression shirt to measure spontaneous breathing. *Biomed Tech,* vol. 62(Suppl.1), p. S127.

Laufer, B., Krueger-Ziolek, S., Docherty, P. D., Hoeflinger, F., Reindl, L., and Moeller, K. (2018). Minimum Number of Sensors in a Smart Shirt to Measure Tidal Volumes. In *10th IFAC Symposium on Biological and Medical Systems BMS 2018*, M. d. Sales and G. Tsuzuki, Eds., (São Paulo, Brazil, 2018), vol. 51, pp. 92-7.

Massaroni, C., Carraro, E., Vianello, A., Miccinilli, S., Morrone, M., Levai, I. K., Schena, E., Saccomandi, P., Sterzi, S.*, et al.* (2017). Optoelectronic Plethysmography in Clinical Practice and Research: A Review. *Respiration,* vol. 93 (5), pp. 339-54.

Miller, M. R., Hankinson, J., Brusasco, V., Burgos, F., Casaburi, R., Coates, A., Crapo, R., Enright, P., van der Grinten, C. P.*, et al.* (2005). Standardisation of spirometry. *Eur Respir J,* vol. 26 (2), pp. 319-38.

Parreira, V. F., Vieira, D. S., Myrrha, M. A., Pessoa, I. M., Lage, S. M., and Britto, R. R. (2012). Optoelectronic plethysmography: a review of the literature. *Rev Bras Fisioter,* vol. 16 (6), pp. 439-53.

Romagnoli, I., Lanini, B., Binazzi, B., Bianchi, R., Coli, C., Stendardi, L., Gigliotti, F., and Scano, G. (2008). Optoelectronic Plethysmography has Improved our Knowledge of Respiratory Physiology and Pathophysiology. *Sensors (Basel, Switzerland),* vol. 8 (12), pp. 7951-72.

Schranz, C., Knobel, C., Kretschmer, J., Zhao, Z., and Moller, K. (2011). Hierarchical Parameter Identification in Models of Respiratory Mechanics. *Biomedical Engineering, IEEE Transactions on,* vol. 58 (11), pp. 3234-41.

Vogiatzis, I., Aliverti, A., Golemati, S., Georgiadou, O., LoMauro, A., Kosmas, E., Kastanakis, E., and Roussos, C. (2005). Respiratory kinematics by optoelectronic plethysmography during exercise in men and women. *European Journal of Applied Physiology,* vol. 93 (5), pp. 581-7.

Yang, G.-Z. (2014). *Body Sensor Networks (2nd ed.)* [Text (nur für elektronische Ressourcen)]. Available: http://dx.doi.org/10.1007/978-1-4471-6374-9
http://swbplus.bsz-bw.de/bsz405478585cov.htm